

# Effectiveness of different transition metal dispersed catalysts for in situ heavy oil upgrading

Almarshed, Abdullah; Hart, Abarasi; Leeke, Gary; Greaves, Malcolm; Wood, Joseph

DOI:

[10.1021/acs.iecr.5b02953](https://doi.org/10.1021/acs.iecr.5b02953)

License:

Creative Commons: Attribution (CC BY)

*Document Version*

Publisher's PDF, also known as Version of record

*Citation for published version (Harvard):*

Almarshed, A, Hart, A, Leeke, G, Greaves, M & Wood, J 2015, 'Effectiveness of different transition metal dispersed catalysts for in situ heavy oil upgrading', *Industrial & Engineering Chemistry Research*, vol. 54, no. 43, pp. 10645–10655. <https://doi.org/10.1021/acs.iecr.5b02953>

[Link to publication on Research at Birmingham portal](#)

## **Publisher Rights Statement:**

Eligibility for repository : checked 16/12/2015

## **General rights**

Unless a licence is specified above, all rights (including copyright and moral rights) in this document are retained by the authors and/or the copyright holders. The express permission of the copyright holder must be obtained for any use of this material other than for purposes permitted by law.

- Users may freely distribute the URL that is used to identify this publication.
- Users may download and/or print one copy of the publication from the University of Birmingham research portal for the purpose of private study or non-commercial research.
- User may use extracts from the document in line with the concept of 'fair dealing' under the Copyright, Designs and Patents Act 1988 (?)
- Users may not further distribute the material nor use it for the purposes of commercial gain.

Where a licence is displayed above, please note the terms and conditions of the licence govern your use of this document.

When citing, please reference the published version.

## **Take down policy**

While the University of Birmingham exercises care and attention in making items available there are rare occasions when an item has been uploaded in error or has been deemed to be commercially or otherwise sensitive.

If you believe that this is the case for this document, please contact [UBIRA@lists.bham.ac.uk](mailto:UBIRA@lists.bham.ac.uk) providing details and we will remove access to the work immediately and investigate.



# Effectiveness of Different Transition Metal Dispersed Catalysts for In Situ Heavy Oil Upgrading

Abdullah Al-Marshed,<sup>†</sup> Abarasi Hart,<sup>†</sup> Gary Leeke,<sup>†</sup> Malcolm Greaves,<sup>‡</sup> and Joseph Wood<sup>\*,†</sup>

<sup>†</sup>School of Chemical Engineering, University of Birmingham, Edgbaston, Birmingham B15 2TT, United Kingdom

<sup>‡</sup>IOR Research Group, Department of Chemical Engineering, University of Bath, Bath BA2 7AY, United Kingdom

## S Supporting Information

**ABSTRACT:** Ultradispersed particles of a size less than 100 nm for in situ catalytic upgrading have been reported to outperform the augmented catalytic upgrading achieved by incorporating pelleted refinery catalyst to the horizontal production well of the toe-to-heel air injection (THAI) process. Hydroconversion of heavy oil was carried out in a stirred batch reactor at 425 °C, 50 bar (initial H<sub>2</sub> pressure), 900 rpm, and 60 min reaction time using a range of unsupported transition metal (Mo, Ni, and Fe) catalysts. The effect of metal nanoparticles (NPs) was evaluated in terms of product distribution, physical properties, and product quality. The produced coke and recovered catalysts were also studied. The levels of API gravity and viscosity of the upgraded oils observed with the NPs was approximately 21° API and 108 cP compared with thermal cracking alone (24° API and 53.5 cP); this moderate upgrade with NPs is due to the lack of cracking functionality offered by supports such as zeolite, alumina, or silica. However, it was found that the presence of dispersed NPs significantly suppressed coke formation: 4.4 wt % (MoS<sub>2</sub>), 5.7 wt % (NiO), and 6.8 wt % (Fe<sub>2</sub>O<sub>3</sub>) compared to 12 wt % obtained with thermal cracking alone. The results also showed that with dispersed unsupported metal NPs in sulfide form the middle distillate (177–343 °C) of the upgraded oil was improved, particularly with MoS<sub>2</sub>, which gave 50 wt % relative to 43 wt % (thermal cracking) and 28 wt % (feed oil). The middle distillate yields for Fe<sub>2</sub>O<sub>3</sub> and NiO are 47 and 49 wt %, respectively. Hence, iron- and nickel-based unsupported NPs showed similar activity when compared to the activity of MoS<sub>2</sub>. The cost and availability of iron-based catalysts compared to those of Ni and Mo for heavy oil upgrading are advantages that may justify its preference. Furthermore, the X-ray diffraction (XRD) and scanning electron microscopy (SEM) analyses showed that introducing dispersed catalysts to the upgrading helped to produce sponge-type coke that could be used as industrial fuel compared to shot-type obtained upon thermal cracking.

## 1. INTRODUCTION

Because of the rapid growth in energy demand worldwide, the world's recoverable fossil energy resources are likely to decline, unless there is significant investment in new oil fields and large scale adoption of advanced enhanced oil recovery (EOR) techniques, combined with increasing efficiency of production. This decline in conventional light crude has shifted attention to large deposits of bitumen and heavy oils especially in Canada.<sup>1,2</sup> Fossil fuels supply around 80% of energy used worldwide.<sup>3</sup> Because conventional crude oil resources have already been extensively exploited and are declining, unconventional oil resources could play an important role in securing the world's future energy needs. However, production, transportation, and upgrading processes of unconventional oil impose different challenges for the oil sector compared with those of conventional oil.<sup>4</sup>

Bitumen and heavy oils are produced mainly by EOR processes because of their poor mobility under reservoir conditions.<sup>5</sup> In this phase, external thermal energy, gas injection, and chemical injection are used to stimulate production. The main goal of thermal EOR is to increase heavy oil recovery by reducing its viscosity. In the case of light oil, the objectives are decreasing interfacial tension and increasing the contact area through the reservoir by improving the sweep efficiency. The application of thermal technology, such as in situ combustion, contributes to reducing the costs of surface upgrading of heavy oil and bitumen.<sup>6</sup>

Steam-assisted gravity drainage (SAGD) and cyclic steam stimulation (CSS) recovery mechanisms depend upon the heat released from injected steam to reduce the viscosity of heavy oil and bitumen to facilitate their mobilization to the surface. In addition, the SAGD method provides a moderate recovery factor of 50% of original oil in place (OOIP), whereas the recovery factor for the CSS method varies from 10 to 40%.<sup>7,8</sup> However, consumption of water and natural gas to generate steam are considered major drawbacks of these methods.<sup>9</sup> Furthermore, the produced oil needs the addition of diluents to facilitate transportation, increasing operational costs.<sup>10</sup> Therefore, in situ combustion can offer operational and economic advantages because heat is generated in situ from the combustion reactions, which aids primary upgrading of the heavy oil and bitumen via thermal cracking of heavy components.

The toe-to-heel air injection (THAI) in combination with the catalytic upgrading process in situ (CAPRI) has been studied extensively for more than 15 years after the first work of Greaves and co-workers.<sup>11–16</sup> The THAI method is classified as a modified in situ combustion because of the use of a horizontal production well, instead of a vertical well, in which air is

**Received:** August 11, 2015

**Revised:** October 1, 2015

**Accepted:** October 7, 2015

**Published:** October 7, 2015

continuously injected to support the in situ combustion, whereas the thermal cracking occurring at the mobile oil zone ahead of the combustion front partially upgrades the oil prior to entering the horizontal well. However, the upgrading achieved with THAI was augmented by CAPRI because of the pelleted catalyst layer attached to the horizontal production well. Further details about the THAI process have been reported elsewhere.<sup>14,17</sup>

A previous study on comparing the upgrading achieved with ultrafine particles and pelleted Co–Mo/Al<sub>2</sub>O<sub>3</sub> catalyst at reaction temperature 425 °C under conditions of the CAPRI process was carried out by Hart et al.<sup>18</sup> The produced oil's API gravity increment and viscosity reduction were found to be 9° points and 96%, respectively, with ultrafine particles, compared to 5° and 79% achieved with pelleted fixed-bed catalyst referred to 13.8° and 1091 cP for the feed heavy oil.<sup>18</sup> However, Galarraga and Pereira-Almao<sup>19</sup> investigated ultradispersed trimetallic (Ni–W–Mo) submicronic catalyst for in situ upgrading at 380 °C in a batch reactor, a stirrer speed of 500 rpm, and reaction time 3–70 h and achieved an API gravity increase of 6.5° and a viscosity reduction of 98% relative to that of Athabasca bitumen (API gravity 9.5° and viscosity 7680 cP). As the size of particle decreases to nanoscale, its specific surface area increases, whereas the diffusion path length decreases. This improves interaction with macromolecules and cracking reaction, increases the probability of active phase interaction with hydrocarbon molecules, improves hydrogen uptake, and leads to more active sites per unit weight. In situ catalytic upgrading with unsupported transition metal particles will minimize coke formation because nanosized catalyst exposes more active sites and possesses short diffusion routes, rather than the diffusion limitation of large molecules experienced in their pelleted counterpart. Because CAPRI is a once-through process, prepacking the horizontal production well with pelleted catalyst is bypassed; the precipitation or transport of the nanoparticles (NPs) into the mobile oil zone ahead of the combustion front is achieved during the THAI process.<sup>18</sup> Also, the possibility of production lines becoming blocked because of coke and metals deposition on the pelleted catalyst is eliminated with dispersed NPs.<sup>2,20</sup>

During heavy oil upgrading, heavy molecules are converted to more valuable product (middle distillate), improving the quality of the produced oil. The cracking of heavy molecules results in the deposition of solid carbonaceous matter and undesired coke.<sup>4</sup> Coke is an undesired product in heavy oil upgrading because it impedes the performance of the catalyst; coke can be classified into three main types: shot-type, sponge-type, and associate-shot-type.<sup>21,22</sup> The chemical compositions of feedstock as well as process operating conditions greatly influence the type of coke formed.<sup>23</sup> Picon-Hernandez et al.<sup>24</sup> reported that sponge-type coke is formed from feedstock that has moderate asphaltene and metal (Ni + V) content.

This paper is devoted to examining the effectiveness and activity of different types of dispersed unsupported transition metal catalysts for in situ heavy oil upgrading instead of packed pellets of catalyst attached to the horizontal well. The sulfidation of the metal oxides during heating and reaction by the sulfur contained in the heavy oil was investigated using Fe<sub>2</sub>O<sub>3</sub> nanoparticles. The performance of molybdenum-, iron-, and nickel-based dispersed catalysts were investigated in terms of product distribution, (i.e., liquid, gas, and coke as well as naphtha, middle distillate, and gas oil fractions), physical properties (i.e., API gravity and viscosity), and product quality

(i.e., sulfur, metals, and nitrogen contents) and evaluated against that achieved with thermal cracking without the addition of metal particles. Also studied herein is the effect of dispersed unsupported catalysts on the type of coke produced from the upgrading reactions using scanning electron microscopy (SEM).

## 2. MATERIAL AND METHODS

**2.1. Feedstock and Catalysts.** A heavy oil sample was supplied by Petrobank Energy and Resources, Ltd., Canada. The heavy oil sample was partially upgraded after being produced during the THAI process at their Whitesands pilot trial in Kerrobert, Canada. The THAI oil was from eight different wells. The chemical and physical properties of the feed sample was measured and are presented in Table S1. The unsupported catalysts used are iron(III) oxide (Fe<sub>2</sub>O<sub>3</sub>) and nickel(II) oxide (NiO), both with particle sizes less than 50 nm, molybdenum(VI) oxide (MoO<sub>3</sub>), with particle size less than 100 nm, molybdenum(IV) sulfide (MoS<sub>2</sub>), with particle size less than 2 μm, and iron(II) sulfide (FeS), with particle size less than 140 μm. All were purchased from Sigma-Aldrich, United Kingdom, and used without further purification.

**2.2. Experimental Apparatus.** The studies to determine the effect of dispersed unsupported catalysts (Mo, Ni, and Fe) on heavy oil upgrading were carried out in a stirred batch reactor (100 mL capacity) in Baskerville, United Kingdom. The batch reactor enabled the screening of an economical quantity of catalysts particles and oil while exercising good control. A detailed description of the experimental setup and procedure can be found in ref 18. The experimental conditions are presented in Table S2.

The stirring speed of 900 rpm was used to ensure complete suspension of the catalysts particles because of the different particle size ranges and the feed oil viscosity. The reaction temperature, initial pressure, and reaction time were optimal conditions found by Hart et al.<sup>18</sup> for the same experimental setup.

**2.3. Analysis of Products.** The main products of the upgrading reactions, upgraded oil (i.e., liquid), noncondensable gas, coke, and asphaltene were quantified by mass balance. The mass balances of gas, liquid, and coke were calculated and reported as a percentage of the mass of oil fed using eq 1:

$$\text{Yield (wt\%)} = \frac{m_i}{m_{\text{feedstockTHAI}}} \times 100 \quad (1)$$

where  $m_i$  is the weight of component  $i$ . The mass of gas produced was calculated as the mass remaining after subtracting the mass of the content of the reactor after reaction. The asphaltene content was determined in accordance with method ASTM D2007-80 using *n*-pentane in order to evaluate the level of heavy oil upgrading.

The feed and collected upgraded oil samples were analyzed for API gravity, viscosity, and true boiling point (TBP) distribution, using the following analytical instruments: an Anton Paar DMA 35 density meter, an Advanced Rheometer AR 1000 (TA Instruments Ltd., United Kingdom), and simulated distillation by Agilent 6850N gas chromatography (GC) in line with the ASTM D2887 method. Note that the calibration mix of the Agilent 6850N GC contains hydrocarbons from C<sub>5</sub> to C<sub>40</sub>. The maximum oven temperature is 280 °C; hence, macromolecules such as resins and asphaltenes outside this carbon range cannot be accounted for by this method. The description of these instruments has been

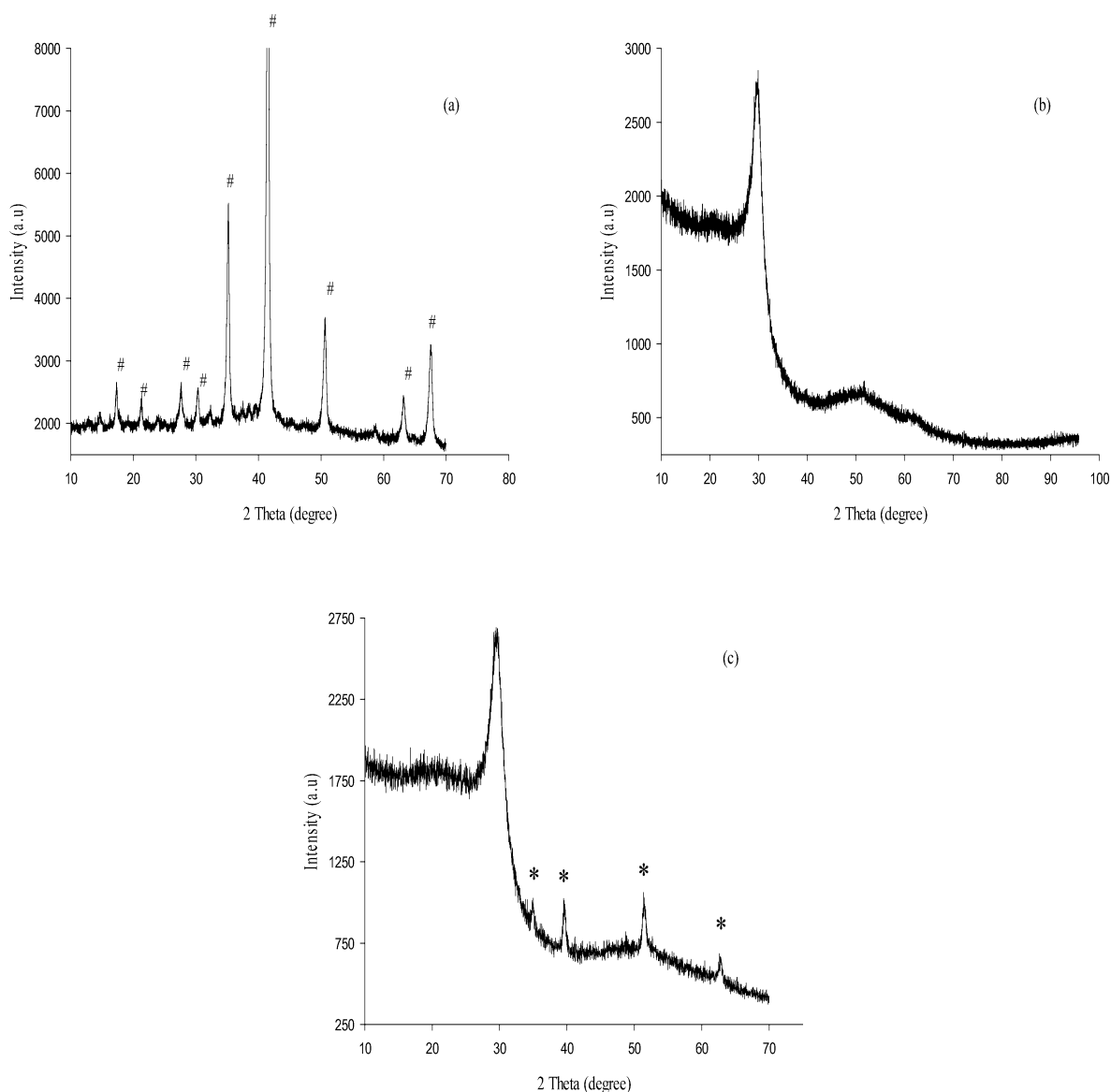


**Figure 1.** XRD pattern for (a) the fresh  $\text{Fe}_2\text{O}_3$  catalysts, (b) recovered coke from thermal upgrading, and (c) recovered coke and catalysts after activation reaction.

reported elsewhere.<sup>25</sup> The sulfur and metal contents of the feed and the upgraded oil samples were determined by Warwick Analytical Service, United Kingdom, using inductively coupled plasma–optical emission spectroscopy (ICP–OES), and nitrogen content was measured by a CE 440 elemental analyzer.

The surface morphology analysis was conducted on the produced coke as well as the spent dispersed catalysts using a Philips XL 30 SEM (XL 30 ESEM-FEG) equipped with a LaB5 emission source operating at 15 kV. A micrograph was collected over a selected area of the sample surface using SEM with a resolution of  $1344 \times 1024$  pixels, width of  $10 \mu\text{m}$ , and magnification of  $35\,000\times$ .

X-ray diffraction (XRD) analysis was conducted using a Bruker D2 PHASER Diffractometer with a scan range from  $0$  to  $160^\circ$  and  $\text{Co K}\alpha$  radiation with a wavelength of  $1.54056 \text{ \AA}$ . The crystalline phase was determined using an EVA database (PDF-4+, 2012) provided by the International Centre for Diffraction Data (ICDD).

### 3. RESULTS AND DISCUSSION

**3.1. Sulfidation Test.** The active phase (metal sulfide) of the dispersed catalysts is formed in situ during the sulfidation reaction between the unsupported metals and the sulfur contained in the heavy oil.<sup>26</sup> This activation process can influence the activity and performance of the dispersed catalysts. The sulfidation reaction was conducted using iron-based dispersed catalysts ( $\text{Fe}_2\text{O}_3$ ). The experiment was carried out without adding a sulfur source at a reaction temperature of  $410^\circ\text{C}$ , 50 bar of initial hydrogen pressure, and 900 rpm mixing speed for 50 min, followed by a reaction temperature of  $425^\circ\text{C}$  for 60 min. The fresh  $\text{Fe}_2\text{O}_3$  and coke from thermal upgrading was analyzed by XRD. In addition, the spent dispersed catalyst was recovered after the sulfidation experiment and analyzed to validate the activation reaction. Figure 1a–c shows the results of XRD analysis of fresh  $\text{Fe}_2\text{O}_3$ , coke (from thermal upgrading), and the recovered coke and catalysts after activation reaction, respectively. The presence of an active-phase pyrrhotite-5C ( $\text{Fe}_{1-x}\text{S}$ ) can be observed. (The obtained



XRD data match with pyrrhotite-5C pattern of the EVA database by ICDD).

Figure 2 shows the SEM micrograph of the recovered coke and iron particles composite after reaction. The iron particle

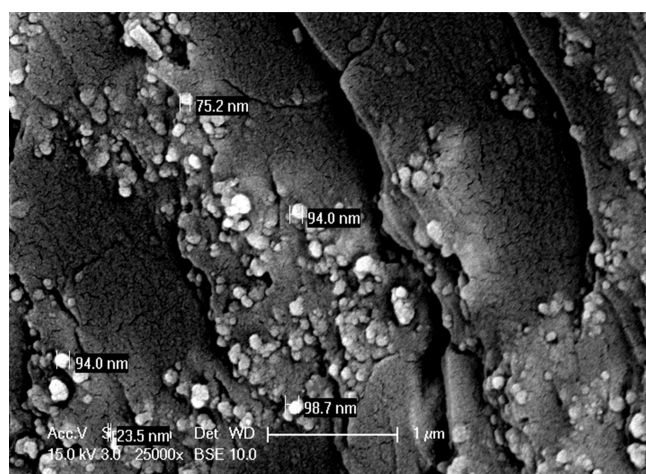


Figure 2. SEM micrograph of recovered  $\text{Fe}_2\text{O}_3$  catalysts.

seen on the SEM image has been identified by XRD (Figure 1c) as pyrrhotite, which has a particle size on the nanometer scale (Figure 2).

It is therefore clear that the unsupported catalysts are converted to their active phase (i.e., activated) during the heating and reaction stage of the experiments as shown in Figure 1c. This procedure and results are consistent with that reported in the literature for activation transition metal catalyst (Mo, Ni, and Fe).<sup>26–29</sup> The sulfidation of Mo and Ni NPs was not carried out because they have been extensively reported in the literature.

**3.2. Effect of Catalyst Size on Heavy Oil Upgrading.** It has been found that the use of ultrafine catalysts could help to mitigate the challenges of coke formation during catalytic upgrading.<sup>30</sup> Stirred-tank reactors have been widely used for the purpose of investigating the effect of dispersed nanocatalysts on hydroconversion of heavy oil.<sup>31,32</sup> The stirring speed used was in line with the guidelines reported in the literature to ensure suspension and adequate dispersion of the particles in the oil during reaction.<sup>33–35</sup> Table 1 shows the effect of particle size on the extent of upgrading for experiments carried out with unsupported  $\text{Fe}_2\text{O}_3$  particles. It can be observed that different particle sizes show similar activity in terms of their effect upon product distribution, physical properties, and product quality of the produced oil at high reaction conditions (described in the footnote for Table 1).

Table 1 shows that the coke yield decreased to 6.76 wt % for  $\text{Fe}_2\text{O}_3$  ( $\leq 50$  nm) and 6.64 wt % for  $\text{Fe}_2\text{O}_3$  ( $\leq 5$   $\mu\text{m}$ ) relative to 12 wt % for thermal upgrading. In addition, the amount of middle distillate fractions increased to 47 wt % for both  $\text{Fe}_2\text{O}_3$  ( $\leq 50$  nm) and  $\text{Fe}_2\text{O}_3$  ( $\leq 5$   $\mu\text{m}$ ) relative to the 28 wt % feedstock. It is well-known that the particle dispersion increases as the stirring speed increases although aggregation could occur at high agitation depending on the viscosity of the feedstock.<sup>36,37</sup> In other words, following high viscosity of the feed oil, both  $\text{Fe}_2\text{O}_3$  ( $\leq 50$  nm) and  $\text{Fe}_2\text{O}_3$  ( $\leq 5$   $\mu\text{m}$ ) could be dispersed adequately at the high mixing speed of 900 rpm, although 500 rpm was found by Hart et al.<sup>18</sup> to be the optimum mixing speed.

Table 1. Effect of Catalyst Size on Product Distribution Physical Properties, and Product Quality<sup>a</sup>

catalyst type/size	non	$\text{Fe}_2\text{O}_3$ ( $\leq 50$ nm)	$\text{Fe}_2\text{O}_3$ ( $\leq 5$ $\mu\text{m}$ )
Product Distribution (wt %)			
coke	12	6.79	6.64
liquid	76	82.48	82.74
gas	12	10.72	10.63
C5-asphaltene	4.5	10	9.89
SIMDIST Boiling Point Distribution (wt %)			
(IBP–177 °C)	25	21	22
(177–343 °C)	43	47	47
(343–525 °C)	32	32	31
Physical Properties			
API gravity at 15 °C	24	21	21.5
viscosity (cP) at 20 °C	53.54	105.75	92
Product Quality Removal %			
HDS	43.92	37.54	35.74
HDM	85.67	69.38	69.29
N (wt %)	0.25	0.14	0.24

<sup>a</sup>Reaction conditions conditions for two steps: (1) 410 °C, 50 min, metal loading 0.1 wt %,  $\text{H}_2$  initial pressure 50 bar, mixing speed 900 rpm; (2) 425 °C, 60 min, mixing speed 900 rpm. Errors are expressed in terms of standard deviation for triplicate experiments as follows: coke wt %  $\pm 0.2$ , liquid wt %  $\pm 0.24$ , gases wt %  $\pm 0.46$ , asphaltene wt %  $\pm 0.8$ , middle distillate (177–343 °C) wt %  $\pm 0.3$ , light naphtha (IBP–177 °C) wt %  $\pm 0.4$ , gas oil (343–525 °C) wt %  $\pm 0.5$ , API°  $\pm 0.28$ , viscosity  $\pm 1.5$ , HDS%  $\pm 0.4$ , metal HDM%  $\pm 0.31$ , N wt %  $\pm 0.03$ . HDS, hydrodesulfurization, and hydrodemetallization, HDM.

The 50 nm particles have a higher surface area/volume ratio than the 5  $\mu\text{m}$  particles, which might be expected to influence their upgrading behavior owing to the different ratio of atomic exposure/surface area; however, it was evident in these two cases that the particle size did not significantly influence the level of upgrading or coke deposit. The lack of influence of the particle size might be expected to occur because of the possible aggregation of the 50 nm particles during the experiment. However, in Figure 2, the SEM of the coke after reaction does not show any evidence for bulk aggregation of the nanoparticles, with individual particles being observed to be distributed across the surface of the coke. Thus, it was concluded that there was no significant overall effect of particle size upon upgrading over the range of particle sizes studied.

**3.3. Effects of Molybdenum-Based Dispersed Catalysts.** Table 2 shows the performance of molybdenum-based catalysts in terms of product distribution, physical properties, and product quality. From Table 2, thermal upgrading (in the absence of catalysts) gave a very high amount of coke and gas and relatively low amounts of liquid and asphaltene. It can be observed that although both light naphtha and middle distillate fractions of the produced oil increased the gas oil fraction decreased after thermal upgrading. The results are in agreement with previous work on thermal upgrading of heavy oil.<sup>4,38</sup> The decrease in the gas oil fraction is an indication that the macromolecules in the heavy feed oil have been cracked into low-boiling hydrocarbon molecules that are in the range of naphtha and middle distillate fractions following their increase.

It is well-known that thermal energy is responsible for the cleavage of C–C and C–heteroatom bonds, and in the absence of active catalysts, the condensation and aromatization reactions between free radicals are favored, which are thought to be responsible for high amounts of coke and gas as well as a relatively low amount of liquid collected compared to that

**Table 2. Effect of Molybdenum-Based Catalysts on Product Distribution, Physical Properties, and Product Quality<sup>a</sup>**

catalyst type/size	non	MoS <sub>2</sub> (<2 μm)	MoO <sub>3</sub> (<100 nm)
Product distribution (wt %)			
coke	12	4.35	5.9
liquid	76	85.84	83.81
gas	12	9.81	10.29
C5-asphaltene	4.5	9.55	7.24
SIMDIST Boiling Point Distribution (wt %)			
(IBP–177 °C)	25	17	21
(177–343 °C)	43	50	49
(343–525 °C)	32	33	30
Physical Properties			
API gravity at 15 °C	24	20	21
viscosity (cP) at 20 °C	53.54	142.38	102.77
Product Quality Removal %			
HDS	43.92	30.55	37.08
HDM	85.67	47.33	68.89
N (wt %)	0.25	0.05	0.2

<sup>a</sup>Reaction conditions for two steps: (1) 410 °C, 50 min, metal loading 0.1 wt %, H<sub>2</sub> initial pressure 50 bar, mixing speed 900 rpm; (2) 425 °C, 60 min, mixing speed 900 rpm. Errors are expressed in terms of standard deviation for triplicate experiments as follows: coke wt % ± 0.15, liquid wt % ± 0.35, gases wt % ± 0.45, asphaltene wt % ± 0.75, middle distillate (177–343 °C) 0.25 wt %, light naphtha (IBP–177 °C) wt % ± 0.45, gas oil (343–525 °C) wt % ± 0.55, API° ± 0.18, viscosity ± 2, HDS% ± 0.55, metal HDM% ± 0.31, N wt % ± 0.01. HDS, hydrodesulfurization, and hydrodemetallization, HDM.

observed upon the addition of an unsupported catalyst.<sup>39,40</sup> At high reaction temperatures, such as 425 °C, the solubility of asphaltene decreases because of the increase in aromatization by removing aliphatic side chains and hydrogenating maltenes (e.g., saturates and aromatics). As a result, the maltenes tend to be more aliphatic, causing precipitation and agglomeration of asphaltene because of their insolubility in aliphatic hydrocarbons.<sup>41–44</sup> The lower content of asphaltene in the produced oil and high yield of coke after thermal upgrading of heavy oil confirmed that large amounts of asphaltene were deposited (Table 2).

In contrast, from Table 2 it can be observed that both molybdenum(IV) sulfide (MoS<sub>2</sub>) and molybdenum(VI) oxide (MoO<sub>3</sub>) dispersed catalysts suppressed coke formation, controlled gas production, and relatively increased the amount of liquid and asphaltene in the produced oil. However, MoS<sub>2</sub> showed activity better than that of MoO<sub>3</sub> for heavy oil upgrading in terms of product distribution. Also, the liquid yield and asphaltene amount increased to 85.84 and 9.55 wt % for MoS<sub>2</sub> and 83.81 and 7.24 wt % for MoO<sub>3</sub>, respectively, relative to 76 and 4.5 wt % in thermal upgrading. The observed lower asphaltene after thermal cracking relative to dispersed unsupported molybdenum catalysts can be attributed to the high carbon rejection caused by high asphaltene deposition during thermal cracking.<sup>41,43–45</sup> Asphaltenes are major coke precursors. Hence, a large precipitation of asphaltene will increase coke yield, whereas the asphaltene content of the liquid phase decreases. Therefore, the presence of metal NPs suppressed the precipitation of asphaltene and coke formation because of their hydrogen-transfer reactions. Hence, thermal cracking produced upgraded oil with lower asphaltene content and high coke yield, whereas upgrading with dispersed metal NPs produced oil with moderate asphaltene content and lower coke yield. Furthermore, the particles lack the cracking

functionality because they are unsupported; hence, the upgrading is mainly by a free radical mechanism with the unsupported catalyst particles aiding hydrogen uptake. On the basis of the distilled fractions, it can be noticed that the presence of molybdenum-based catalysts increased the amount of valuable middle distillate, whereas the light naphtha fraction decreased relative to that of thermal cracking without catalyst addition (Table 2).

A similar level of upgrading in terms of product distribution was observed for Mo-based dispersed catalysts and reported in the literature.<sup>38,46–48</sup> Also, in the hydroconversion investigation of Cold Lake vacuum residue at 415–445 °C, 13.8 MPa, and a reaction time of 1 h, Rezaei et al.<sup>49</sup> found that utilizing MoS<sub>2</sub> suppressed coke formation from 22 wt % in the absence of catalysts (i.e., thermal cracking) to 4.8 wt % in the presence of 100 ppm of Mo. This significant suppression of coke formation could be attributed mainly to hydrogen uptake, which is a major function of the unsupported catalyst particles.<sup>50</sup> The hexagonal coordination exhibited by unsupported MoS<sub>2</sub> contributed to its activity.<sup>50–52</sup> During hydroprocessing reactions, the corner and edge that are active sites occupied by sulfur ions in MoS<sub>2</sub> could be easily interchanged with hydrogen. As a result, unsaturated sites and sulfur ion vacancies formed that exhibit Lewis acid characteristics and active sites for H<sub>2</sub>. The activation of H<sub>2</sub> on the surface of the catalyst particles therefore form Mo–H and S–H moieties that helped to decrease the rate of condensation and aromatization reactions by hydrogenated free radicals.<sup>50,53,54</sup> As a consequence, the following was observed upon the addition unsupported Mo-based particles to the heavy oil upgrading: (1) suppression of coke formation, (2) control of gas formation, and (3) improvement of production of the middle distillate fraction.

Table 2 also shows the effect of Mo-based catalysts on physical properties as well as product quality. High viscosity and low API gravity causes major problems during the extraction and transportation process.<sup>55</sup> Low API gravity and high viscosity for heavy oil could be attributed to high average molecular weight fractions (such as asphaltene) and the interaction strength between molecules.<sup>56–58</sup> An increase in temperature accelerates the rate of major reactions occurring in the slurry environment such as free radical formation from C–C and C–heteroatom bond cleavage.<sup>12,59,60</sup> As a consequence of molecular bond cleavage and the rupture of ring structures of heavy oil, gas, coke, and large numbers of smaller and less viscous products form.<sup>55,56</sup>

The experiment on thermal upgrading of heavy oil has demonstrated that the viscosity falls drastically to 54 cP and API gravity increases to 24° relative to 1482 cP and 12.8°, respectively, for the feed oil. In contrast, it has been noticed that after upgrading with Mo-based dispersed catalysts (MoS<sub>2</sub> and MoO<sub>3</sub>) the produced oil did not have the same level of improvements in both API gravity and viscosity as those observed with thermal upgrading. The API gravity and viscosity were observed to be 20° and 142.38 cP for MoS<sub>2</sub> and 21.3° and 99.9 cP for MoO<sub>3</sub>, respectively. Nevertheless, Hart et al.<sup>18</sup> found a 8.7° increase in API gravity with ultradispersed Co–Mo/Al<sub>2</sub>O<sub>3</sub> versus 6.6° increase with thermal cracking. The difference is that their catalyst (Co–Mo/Al<sub>2</sub>O<sub>3</sub>) possesses bifunctionality (i.e., cracking by the alumina support and hydrogenation by the dispersed Co–Mo). It has also been reported in the literature<sup>45,56,61–63</sup> that unsupported catalysts such as those used in this study (e.g., MoS<sub>2</sub>) are not bifunctional in nature because they do not promote cracking

of C–C and C–heteroatom bonds by the acidic sites present on zeolites and alumina. Further cracking was not therefore experienced with the addition of the unsupported catalyst because the main mechanism of upgrading is by free radical driven temperature. The unsupported catalyst carried out hydrogenation that helped to stabilize asphaltene in the reaction medium, explaining the decrease of API gravity as well as the higher viscosity relative to thermal cracking.<sup>41,64</sup> This is again consistent with the high asphaltene content of the produced oil after upgrading with unsupported catalysts compared to thermal cracking.

To evaluate the performance of Mo-based catalysts, the product quality in terms of sulfur, nitrogen, and metal removal was investigated and is presented in Table 2. It can be seen from Table 2 that the extent of hydrodesulfurization (HDS) and hydrodemetallization (HDM) is directly proportional to coke yield. This is because the sulfur and metals are associated with macromolecules such as resins and asphaltenes that are the main contributors to coke formation. In the absence of the unsupported catalysts, HDS and HDM were 43.92 and 85.67%, respectively. However, in the presence of dispersed unsupported catalysts, the HDS and HDM decreased to 30.55 and 47.33% for MoS<sub>2</sub> and 37.08 and 68.89% for MoO<sub>3</sub>, respectively. This observation is because of the high coke observed with thermal cracking. It is known that hydrogen plays a key role in HDM reactions.<sup>65–67</sup> Panariti et al.<sup>28</sup> observed that a high initial hydrogen pressure (160 bar) strongly affected metal removal during heavy oil upgrading using unsupported MoS<sub>2</sub>. In the presence of hydrogen, organometallic molecules decompose quite easily, giving rise to insoluble metal sulfide. In another study, Panariti et al.<sup>68</sup> showed that HDS is not affected much by a high initial H<sub>2</sub> pressure; however, HDS was significantly improved at a high level of catalyst loading. The above findings indicate that the breaking of the C–heteroatom bond is mainly controlled by temperature to overcome the bond energy. In addition, the presence of highly active unsupported catalysts can help in stabilizing macromolecules such as asphaltene that act as stores for the sulfur and metals (Ni + V) in the reaction medium.<sup>41,43</sup> Notably, the level of HDM was higher than that of HDS because the concentration of sulfur in the feed oil was higher than that of the metals; additionally, metals are associated mainly with macromolecules such as asphaltenes, whereas sulfur can exist as sulfide, disulfide, and thiol.

The nitrogen content increased to 0.25 and 0.2 wt % for thermal upgrading and MoO<sub>3</sub>, respectively. These results are consistent with the literature, where Gray et al.<sup>69</sup> reported that nitrogen compounds such as pyrroles are much less reactive, which can lead to the accumulation of nitrogen compounds during the upgrading process. However, MoS<sub>2</sub> reduced the nitrogen amount by 46% to below 0.08 wt % in feed oil. Under hydroconversion conditions, MoS<sub>2</sub> catalysts can form unsaturated sites and sulfur ion vacancies. These have Lewis acid characteristics that could adsorb molecules with unpaired electrons (e.g., N bases) in the feed oil.<sup>50</sup> In summary, molybdenum-based dispersed catalysts inhibit coke formation as well as boost production of middle distillate during heavy oil upgrading by activating the hydrogenation reactions. However, MoS<sub>2</sub> and MoO<sub>3</sub> catalysts show different levels of upgrading in terms of product distribution, physical properties, and product quality. It has been observed<sup>27,70–73</sup> that the transformation of MoO<sub>3</sub> to the active phase (MoS<sub>2</sub>) during the heating and reaction stage could be affected by a reducing atmosphere such

as temperature and sulfur content. Feldman et al.<sup>73</sup> and Nath et al.<sup>71</sup> reported that if the reduction atmosphere is not sufficient then it could lead to the formation of an associate intermediate such as MoO<sub>2-x</sub>S<sub>x</sub> which is less active in comparison to MoS<sub>2</sub>. This is likely the reason for the better performance of MoS<sub>2</sub> over MoO<sub>3</sub>.

**3.4. Effect of Fe-Based Catalysts.** Pyrite (FeS<sub>2</sub>), troilite (FeS), and pyrrhotite (Fe<sub>1-x</sub>S) are the most common iron sulfides, and among all of these, the most active form is pyrrhotite (Fe<sub>1-x</sub>S).<sup>74–76</sup> Under hydroprocessing conditions, iron oxide (i.e., Fe<sub>2</sub>O<sub>3</sub>) can be converted to the sulfide form via the reaction with sulfur in heavy oil as shown in Figures 1 and 2. Hydrogen molecules are believed to be activated because of sulfur-deficient sites in iron sulfide catalysts.<sup>77</sup> The active hydrogen can help in terminating condensation and polymerization reactions between free radicals. As a consequence, valuable products such as middle distillate increased, and coke formation was inhibited in comparison to that resulting from thermal cracking.

Table 3 shows the activity of Fe-based dispersed catalysts on heavy oil upgrading in terms of product distribution, product

**Table 3. Effect of Iron-Based Catalysts on Product Distribution, Physical Properties, and Product Quality<sup>a</sup>**

catalyst type/size	non	Fe <sub>2</sub> O <sub>3</sub> (≤50 nm)	FeS (≤140 μm)
Product Distribution (wt %)			
coke	12.0	6.79	8.28
liquid	76.0	82.48	81.9
gas	12	10.72	9.83
C5-asphaltene	4.5	10	7.26
SIMDIST Boiling Point Distribution (wt %)			
(IBP–177 °C)	25	21	24
(177–343 °C)	43	47	48
(343–525 °C)	32	32	28
Physical Properties			
API gravity at 15 °C	24	21	21
viscosity (cP) at 20 °C	53.5	105.8	102.8
Product Quality Removal %			
HDS	43.9	37.5	39.6
HDM	85.7	69.4	75.2
N (wt %)	0.25	0.14	0.2

<sup>a</sup>Reaction conditions for two steps: (1) 410 °C, 50 min, metal loading 0.1 wt %, H<sub>2</sub> initial pressure 50 bar, mixing speed 900 rpm; (2) 425 °C, 60 min, mixing speed 900 rpm. Errors are expressed in terms of standard deviation for triplicate experiments as follows: coke wt % ± 0.3, liquid wt % ± 0.19, gases wt % ± 0.6, asphaltene wt % ± 0.85, middle distillate (177–343 °C) wt % ± 0.4, light naphtha (IBP–177 °C) wt % ± 0.35, gas oil (343–525 °C) wt % ± 0.45, API° ± 0.28, viscosity ± 2, HDS% ± 0.65, metal HDM% ± 0.38, N wt % ± 0.02. HDS, hydrodesulfurization, and hydrodemetallization, HDM.

quality, and physical properties. It has been shown in section 3.2 and Table 2 that unsupported Fe-based catalysts give similar levels of upgrading at 900 rpm under the same experimental conditions. The coke decreased from 12 wt % for thermal cracking without catalyst to 8.28 wt % for FeS and 6.79 wt % for Fe<sub>2</sub>O<sub>3</sub>. In addition, the produced gas yields were 9.59 wt % for FeS and 10.72 wt % for Fe<sub>2</sub>O<sub>3</sub>. Also, in comparison to thermal upgrading, an increase was observed for the liquid amount at 81.9 wt % for FeS and at 82.48 wt % for Fe<sub>2</sub>O<sub>3</sub>.

The distilled fractions from the SimDist analysis showed the following results for FeS: light naphtha, 24 wt %; middle distillate, 48 wt %; and gas oil, 28 wt %. However, for Fe<sub>2</sub>O<sub>3</sub>,



the distillate fraction increased to 47 wt %, the light naphtha fraction reduced to 21 wt %, and the gas oil fraction stayed constant at 32 wt %. These results are in line with the literature, where similar observations have been reported.<sup>74,78,79</sup> It was observed that the asphaltene amount in the produced oil was 7.3 wt % for FeS and 10 wt % for Fe<sub>2</sub>O<sub>3</sub>, relative to 4.5 wt % in thermal upgrading. This finding is consistent with the observation for MoS<sub>2</sub> and MoO<sub>3</sub>, as discussed in section 3.3.

Table 3 shows the performance of Fe-based catalysts in terms of physical properties and product quality. As expected, the results did not show further improvement in terms of physical properties or product quality when using Fe-based catalyst relative to those obtained via thermal upgrading. However, coke formation was suppressed significantly by 43.4% (Fe<sub>2</sub>O<sub>3</sub>) and 31.1% (FeS), which is in line with that observed with Mo-based catalysts. An API gravity of 21° and a viscosity of 102.8 ± 2 cP were observed for produced oil with FeS and Fe<sub>2</sub>O<sub>3</sub> relative to 24° and 53 cP achieved with thermal upgrading. In addition, the extent of sulfur (HDS) and metal (HDM) removal was, respectively, 39.6 and 75.2% for FeS and 37.5 and 69.4% for Fe<sub>2</sub>O<sub>3</sub>. Although FeS showed HDS activity slightly higher than that of Fe<sub>2</sub>O<sub>3</sub>, the reverse was the case for HDM. The trend is similar to that reported in section 3.3, and the HDM is consistent with coke yield (Table 3). However, Fe-based unsupported catalysts showed behavior similar to that of MoO<sub>3</sub> in terms of removal of nitrogen. The nitrogen content was 0.2 wt % (FeS) and 0.14 wt % (Fe<sub>2</sub>O<sub>3</sub>), and these results are similar to those of Gray et al.<sup>69</sup>

The observed overall performance of Fe-based catalysts was similar to that of Mo-based counterparts in terms of API gravity, viscosity, distillate fractions, HDS, and HDM; however, Mo-based unsupported catalysts showed higher activity in suppressing coke formation. These results show the effectiveness of Fe-based unsupported catalysts as an attractive and alternative choice for in situ heavy oil upgrading when cost and availability are considered.

**3.5. Nickel-Based Catalysts.** It has been shown that unsupported metal oxide catalysts are converted to their sulfide form during heating and reaction (section 3.1) and that the performance of oxide and sulfide forms were approximately similar (sections 3.3 and 3.4).

Table 4 shows the performance of nickel-based catalysts in terms of product distribution, physical properties, and product quality. It can be seen that NiO-dispersed catalysts gave a low amount of coke, a moderate amount of gas, and a relatively high amount of liquid and asphaltene.

The product distributions achieved are as follows: coke, 5.8 wt %; gas, 9.5 wt %; liquid, 84.6 wt %; and asphaltene, 8.6 wt %. Notably, both light naphtha and the middle distillate fraction increased, whereas the gas oil fraction decreased in comparison to that achieved via thermal upgrading. The coke yield was reduced remarkably in a manner similar to that of the Mo unsupported catalyst. Zhang et al.<sup>30</sup> reported that coke yield is significantly inhibited using dispersed nickel catalysts at 425 °C, 6 MPa, Ni loading of 300 µg/g, and a reaction time of 1 h during residue hydrocracking. This is because the active metals (Ni, Mo, or Fe) help to moderate the rate of free radical propagation via  $\beta$ -scission reactions by incorporating hydrogen to the cracked active hydrocarbon fragments during heavy oil upgrading.<sup>60,80</sup> This would explain the decrease in coke formation as well as the increase in liquid amount during hydroconversion in the presence of unsupported metal catalysts.<sup>81,82</sup> The distillate fractions of the produced oil after

**Table 4. Effect of Nickel-Based Catalysts on Product Distribution, Physical Properties, and Product Quality<sup>a</sup>**

catalyst type/size	non	NiO (≤50 nm)
Product Distribution (wt %)		
coke	12	5.76
liquid	76	84.64
gas	12	9.59
C5-asphaltene	4.5	8.58
SIMDIST Boiling Point Distribution (wt %)		
(IBP–177 °C)	25	21
(177–343 °C)	43	49
(343–525 °C)	32	30
Physical Properties		
API gravity at 15 °C	24	22.4
viscosity (cP) at 20 °C	53.54	74.12
Product Quality Removal %		
HDS	43.92	35.08
HDM	85.67	65.37
N (wt %)	0.25	0.14

<sup>a</sup>Reaction conditions for two steps: (1) 410 °C, 50 min, metal loading 0.1 wt %, H<sub>2</sub> initial pressure 50 bar, mixing speed 900 rpm; (2) 425 °C, 60 min, mixing speed 900 rpm. Errors are expressed in terms of standard deviation for triplicate experiments as follows: coke wt % ± 0.17, liquid wt % ± 0.36, gases wt % ± 0.5, asphaltene wt % ± 0.67, middle distillate (177–343 °C) wt % ± 0.23, light naphtha (IBP–177 °C) wt % ± 0.54, gas oil (343–525 °C) wt % ± 0.25, API° ± 0.3, viscosity ± 2.7, HDS% ± 0.35, metal HDM% ± 0.45, N wt % ± 0.02. HDS, hydrodesulfurization, and hydrodemetallization, HDM.

upgrading with unsupported Ni catalyst were 21 wt % (light naphtha), 49 wt % (middle distillate), and 30 wt % (gas oil). These results are in agreement with the literature.<sup>28,30</sup>

From Table 4 it can be observed that the upgraded oil with Ni catalyst produced more middle distillate than that achieved with thermal cracking. However, a reverse trend was seen for the naphtha fraction, whereas gas oil is similar within a marginal error of ±0.3% (standard deviation).

The upgraded oil after experiments with NiO particles achieved a viscosity value of 74.12 cP and an API gravity increase to 22.4° relative to 1482 cP and 12.8°, respectively, for the feed oil. However, in comparison to thermal upgrading, the results did not show higher improvement in API gravity and viscosity (Table 4). This is consistent with previous observations on the use of Mo and Fe unsupported catalysts discussed in sections 3.3 and 3.4. The low API gravity and high viscosity of produced oil after upgrading with Ni catalyst can be attributed to the high average molecular weight fractions (such as asphaltene) and the interaction strength between molecules.<sup>56–58</sup> The absence in cracking functionality of the unsupported metal particles contributed to this observation.

Table 4 also shows the effect of nickel oxide (NiO) dispersed catalysts on the removal of sulfur, metal, and nitrogen. The immediate evaluation showed no further improvement in comparison to thermal upgrading. The HDS and HDM obtained was 35.1 and 65.4%, respectively, for NiO in comparison to 43.9 and 85.7%, respectively, for thermal upgrading. It has been reported that the breaking of the C–heteroatom bond is mainly controlled by temperature.<sup>35,81</sup> In addition, under reaction conditions Ni-based catalysts could be converted to sulfide phase (NiS and Ni<sub>3</sub>S<sub>4</sub>).<sup>81,83</sup> Nickel-based catalysts in their sulfide form are considered to be highly active for hydrogen activation, therefore, hydrogenating free radicals during heavy oil upgrading.<sup>70</sup> In terms of nitrogen removal, Ni-



based catalysts showed behavior similar to that of  $\text{MoO}_3$  and  $\text{Fe}_2\text{O}_3$ . The nitrogen content increased to 0.14 wt % for NiO relative to 0.08 wt % in the feed oil. A detailed explanation has been provided in sections 3.3 and 3.4. However, NiO has very similar activity effectiveness in comparison to the metal oxides of Mo and Fe.

**3.6. Effect of Dispersed Catalysts on Type of Formed Coke.** The spent metal NPs was highly encapsulated with coke from cracked hydrocarbon molecules and asphaltenes. However, the spent metal NPs can be recovered if magnetic characteristics can be induced, which is outside the scope of this study. There is a body of research directed to increase coke market value for use applications such as industrial fuel or making anodes for aluminum manufacturing.<sup>84,85</sup> A morphological investigation was conducted on coke samples obtained from thermal and unsupported catalytic upgrading in order to identify the coke quality and type.

Figure 3a,b shows the SEM photomicrographs of coke recovered after thermal upgrading. It can be observed that the

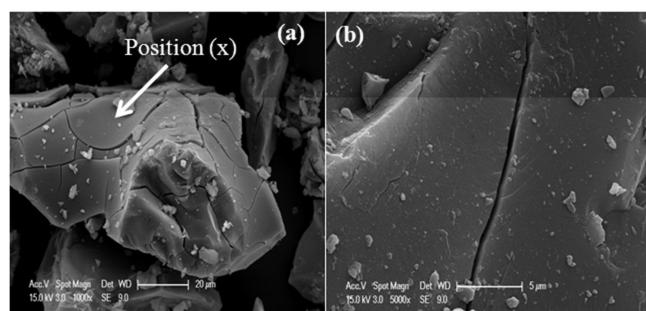


**Figure 3.** SEM photomicrograph of recovered coke after thermal cracking upgrading at (a) 1000 $\times$  magnification and (b) 5000 $\times$  magnification. (For reaction conditions, see Table 2).

coke texture is characterized by a smooth and concave surface (position x in Figure 3a) with no evidence of holes. From a morphological standpoint, the coke produced by thermal upgrading could be classified as shot-type coke, and other researchers have made similar observations in the literature.<sup>21–23</sup>

In addition, it has been reported that the type of coke formed is mainly dependent on feed properties; in particular, high asphaltene and metal content leads to shot-type coke.<sup>22,24,86</sup> This can also be affected by low-temperature oxidation (LTO), producing shiny, very hard, and more difficult to burn coke. This therefore confirmed the high level of metal removal and low asphaltene content of the produced oil observed with thermal cracking (Tables 1 and 2). In a similar light, Picon-Hernandez et al.<sup>24</sup> observed that shot-type coke from coking processes of feed oil has an asphaltene amount of 14 wt % as well as 600 ppm of metal (Ni + V) content. The asphaltene stability in the oil mixture could be disturbed during thermal upgrading,<sup>41</sup> which could lead to precipitation of asphaltene and promote shot-type coke formation.<sup>21</sup> The asphaltene and metal contents of the feed oil used in this study were 14 and 0.0132 wt % (132 ppm), respectively, previously shown in Table S1, which has the tendency to form shot-type coke. Shot-type coke is low in economic value and consists of individual particles that are spherical to slightly ellipsoidal, with average diameters of about 1–4 mm.<sup>21</sup> Nevertheless, understanding feed properties as well as controlling upgrading reaction conditions can help in minimizing low-value coke (shot-type

coke) and in producing more economically valuable coke types.<sup>23</sup>

Figures 4 and 5 show the SEM photomicrographs for the coke recovered after upgrading using dispersed unsupported

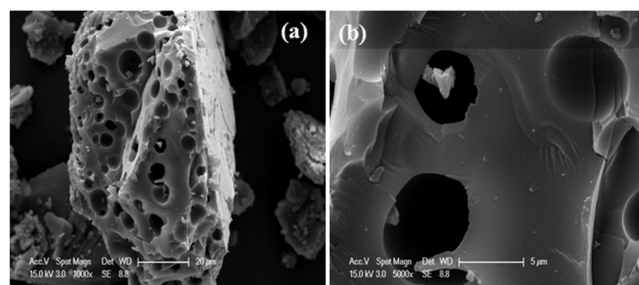


**Figure 4.** SEM photomicrograph of recovered coke after catalytic upgrading with NPs of  $\text{MoS}_2$  at different magnification: (a) 1000 $\times$  and (b) 5000 $\times$ .

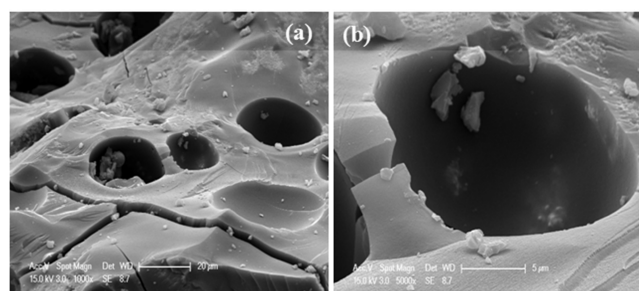


**Figure 5.** SEM photomicrograph of recovered coke after catalytic upgrading with NPs of  $\text{Fe}_2\text{O}_3$  at different magnification: (a) 1000 $\times$  and (b) 5000 $\times$ .

catalysts  $\text{MoS}_2$  and  $\text{Fe}_2\text{O}_3$ , respectively; for reaction conditions, see Tables 2 and 3. Similar micrographs were obtained for NiO,  $\text{MoO}_3$ , and FeS catalysts (not shown).

It is clear from Figures 4 and 5 that the coke texture is characterized by a highly porous microstructure with a wide variety of pore sizes. From a morphological standpoint, the coke produced after upgrading reactions using unsupported metals catalysts such as  $\text{MoS}_2$  and  $\text{Fe}_2\text{O}_3$  can be classified as sponge-type coke. Similar observations have been reported elsewhere.<sup>24,86</sup> Sponge-type coke is named for its spongelike appearance with different sized pores and bubbles in the coke matrix. Compared to shot-type coke observed for coke produced after thermal cracking (Figure 3), sponge-type coke has a higher economic value with a high potential to be used as fuel.<sup>85</sup> It was observed that the asphaltene content in feed oil is the main factor responsible for shot-type coke versus sponge-type coke formation in delayed cokers.<sup>21,85,86</sup> Moreover, Picon-Hernandez et al.<sup>24</sup> observed sponge-type coke from coking processes of feed oil, which moderated asphaltene and metal (Ni + V) content. It can therefore be confirmed that the active metal (Ni, Mo, or Fe) actually helped in controlling the rate of addition reactions between free radicals during heavy oil upgrading by promoting hydrogen uptake by the cracked active hydrocarbon fragments.<sup>60,80</sup> This stabilizes the asphaltene in the oil mixture and explains the formation of sponge-type coke during catalytic upgrading with  $\text{MoS}_2$  and  $\text{Fe}_2\text{O}_3$ . Furthermore, sponge-type cokes are porous lumps that are surrounded by relatively thin walls with no interconnection between pores.<sup>87,88</sup> In the reservoir, the flow of upgraded oil could crack and

convey sponge-type coke to the production well and to the surface because of its physical appearance. Coke laid down ahead of the combustion front during the THAI process acts as fuel for the process.

#### 4. CONCLUSIONS

In this study, the effect of different types of transition metals dispersed catalysts for in situ catalytic upgrading of heavy oil during the THAI heavy oil recovery process was investigated in a stirred batch reactor. It was found that the dispersed catalysts (Ni, Mo, and Fe) in sulfide form could enhance hydrogen uptake and help in controlling the rate of free radical propagation via  $\beta$ -scission reactions during heavy oil upgrading. Despite the improved API gravity and viscosity of the produced oil (24° and 54 cP) by thermal cracking over that achieved with unsupported metal catalyst (approximately 21° and 108 cP), thermal cracking gave a lower amount of upgraded oil (76 wt %) compared to an average of 83.5 wt % for dispersed catalysts. Thermal cracking also yielded 12 wt % coke, whereas the coke yields for dispersed unsupported catalysts are remarkably lower at 4.35 wt % (Mo catalyst), 5.76 wt % (Ni catalyst), and 6.79 wt % (Fe catalyst). The high coke yield with thermal cracking contributed significantly to sulfur and metal (Ni + V) removal because they mostly associate with macromolecules such as resins and asphaltenes, which are the major coke precursors. This is confirmed from the lower asphaltene content of the upgraded oil after thermal cracking compared to catalytic upgrading with dispersed unsupported Fe, Mo, and Ni metals. However, unsupported Mo catalysts showed higher activity in suppressing coke formation and improved middle distillate levels compared to those of Ni and Fe catalysts. Also, the presence of dispersed catalysts helped in producing sponge-type coke compared to shot-type coke from thermal cracking.

#### ■ ASSOCIATED CONTENT

##### Supporting Information

The Supporting Information is available free of charge on the ACS Publications website at DOI: 10.1021/acs.iecr.5b02953.

Properties of heavy oil feedstock and experimental conditions. (PDF)

#### ■ AUTHOR INFORMATION

##### Corresponding Author

\*Tel.: +44 (0) 1214145295. Fax: +44 (0) 1214145324. E-mail: J. Wood@bham.ac.uk.

##### Notes

The authors declare no competing financial interest.

#### ■ ACKNOWLEDGMENTS

We acknowledge the financial support of Kuwait Institute for Scientific Research (KISR), Kuwait, EPSRC, United Kingdom (grant nos. EP/E057977/1 and EP/J008303/1), and Petrobank Energy and Resources, Ltd., Canada (now Touchstone Exploration, Inc.) for supplying the heavy crude oil used in this study. The sulfur and metals analysis was carried out by Warwick Analytical Service, University of Warwick Science Park, United Kingdom. Data sets regarding this publication are available online free of charge via <http://epapers.bham.ac.uk/>.

#### ■ REFERENCES

(1) Hofmann, H.; Babadagli, T.; Zimmermann, G. Hot water generation for oil sands processing from enhanced geothermal

systems: Process simulation for different hydraulic fracturing scenarios. *Appl. Energy* **2014**, *113*, 524–547.

(2) Hashemi, R.; Nassar, N. N.; Pereira Almaso, P. Nanoparticle technology for heavy oil in-situ upgrading and recovery enhancement: Opportunities and challenges. *Appl. Energy* **2014**, *133*, 374–387.

(3) Martínez-Palou, R.; Mosqueira, M. d. L.; Zapata-Rendón, B.; Mar-Juárez, E.; Bernal-Huicochea, C.; de la Cruz Clavel-López, J.; Aburto, J. Transportation of heavy and extra-heavy crude oil by pipeline: A review. *J. Pet. Sci. Eng.* **2011**, *75*, 274–282.

(4) Carrillo, J. A.; Corredor, L. M. Upgrading of heavy crude oils: Castilla. *Fuel Process. Technol.* **2013**, *109*, 156–162.

(5) Bera, A.; Babadagli, T. Status of electromagnetic heating for enhanced heavy oil/bitumen recovery and future prospects: A review. *Appl. Energy* **2015**, *151*, 206–226.

(6) Komery, D. P.; Luhning, R. W.; O'Rourke, J. C. Towards commercialization of the UTF project using surface drilled horizontal SAGD wells. *J. Can. Pet. Technol.* **1999**, *38*, 36–43.

(7) Zhao, D. W.; Wang, J.; Gates, I. D. Thermal recovery strategies for thin heavy oil reservoirs. *Fuel* **2014**, *117*, 431–441.

(8) Yee, C. T.; Stroich, A. Flue gas injection into a mature SAGD steam chamber at the Dover Project (formerly UTF). *J. Can. Pet. Technol.* **2004**, *43*, 54–61.

(9) Giacchetta, G.; Leporini, M.; Marchetti, B. Economic and environmental analysis of a Steam Assisted Gravity Drainage (SAGD) facility for oil recovery from Canadian oil sands. *Appl. Energy* **2015**, *142*, 1–9.

(10) Gates, I. D. Oil phase viscosity behaviour in Expanding-Solvent Steam-Assisted Gravity Drainage. *J. Pet. Sci. Eng.* **2007**, *59*, 123–134.

(11) Xia, T. X.; Greaves, M. Upgrading Athabasca tar sand using toe-to-heel air injection. *J. Can. Pet. Technol.* **2002**, *41*, 51–57.

(12) Hart, A.; Leeke, G.; Greaves, M.; Wood, J. Down-hole heavy crude oil upgrading by CAPRI: Effect of hydrogen and methane gases upon upgrading and coke formation. *Fuel* **2014**, *119*, 226–235.

(13) Greaves, M.; Dong, L. L.; Rigby, S. P. Simulation Study of the Toe-to-Heel Air Injection Three-Dimensional Combustion Cell Experiment and Effects in the Mobile Oil Zone. *Energy Fuels* **2012**, *26*, 1656–1669.

(14) Xia, T. X.; Greaves, M. In situ upgrading of Athabasca Tar Sand bitumen using THAI. *Chem. Eng. Res. Des.* **2006**, *84*, 856–864.

(15) Xia, T. X.; Greaves, M.; Turta, A. T.; Ayasse, C. THAI—A 'Short-Distance Displacement' In Situ Combustion Process for the Recovery and Upgrading of Heavy Oil. *Chem. Eng. Res. Des.* **2003**, *81*, 295–304.

(16) Greaves, M.; El-Saghr, A.; Xia, T. X. CAPRI horizontal well reactor for catalytic upgrading of heavy oil. *Prepr.-Am. Chem. Soc., Div. Pet. Chem.* **2000**, *45*, 595–598.

(17) Shah, A.; Fishwick, R.; Wood, J.; Leeke, G.; Rigby, S.; Greaves, M. A review of novel techniques for heavy oil and bitumen extraction and upgrading. *Energy Environ. Sci.* **2010**, *3*, 700–714.

(18) Hart, A.; Greaves, M.; Wood, J. A comparative study of fixed-bed and dispersed catalytic upgrading of heavy crude oil using-CAPRI. *Chem. Eng. J.* **2015**, DOI: 10.1016/j.cej.2015.01.101.

(19) Galarraga, C. E.; Pereira-Almaso, P. Hydrocracking of Athabasca bitumen using submicronic multimetallic catalysts at near in-reservoir conditions. *Energy Fuels* **2010**, *24*, 2383–2389.

(20) Krishnamoorti, R. Extracting the benefits of nanotechnology for the oil industry. *JPT, J. Pet. Technol.* **2006**, *58*, 24.

(21) Siskin, M.; Kelemen, S. R.; Gorbaty, M. L.; Ferrughelli, D. T.; Brown, L. D.; Eppig, C. P.; Kennedy, R. J. Chemical Approach to Control Morphology of Coke Produced in Delayed Coking. *Energy Fuels* **2006**, *20*, 2117–2124.

(22) Kelemen, S. R.; Siskin, M.; Gorbaty, M. L.; Ferrughelli, D. T.; Kwiatek, P. J.; Brown, L. D.; Eppig, C. P.; Kennedy, R. J. Delayed Coker Coke Morphology Fundamentals: Mechanistic Implications Based on XPS Analysis of the Composition of Vanadium- and Nickel-Containing Additives during Coke Formation. *Energy Fuels* **2007**, *21*, 927–940.

(23) Elliott, J. D. Shot coke: Design & operations. *Today's Refinery* **2000**, *15*, 1–9.



- (24) Picón-Hernández, H.-J.; Centeno-Hurtado, A.; Pantoja-Agreda, E.-F. Morphological classification of coke formed from the castilla and jazmín crude oils. *CTF Cienc. Tecnol. Futuro* **2008**, *3*, 169–183.
- (25) Hart, A.; Shah, A.; Leeke, G.; Greaves, M.; Wood, J. Optimization of the CAPRI Process for Heavy Oil Upgrading: Effect of Hydrogen and Guard Bed. *Ind. Eng. Chem. Res.* **2013**, *52*, 15394–15406.
- (26) Liu, D.; Kong, X.; Li, M. Y.; Que, G. H. Study on a Water-Soluble Catalyst for Slurry-Phase Hydrocracking of an Atmospheric Residue. *Energy Fuels* **2009**, *23*, 958–961.
- (27) Ren, R.; Wang, Z.; Guan, C.; Shi, B. Study on the sulfurization of molybdate catalysts for slurry-bed hydroprocessing of residuum. *Fuel Process. Technol.* **2004**, *86*, 169–178.
- (28) Panariti, N.; Del Bianco, A.; Del Piero, G.; Marchionna, M. Petroleum residue upgrading with dispersed catalysts: Part 1. Catalysts activity and selectivity. *Appl. Catal., A* **2000**, *204*, 203–213.
- (29) Bhattacharyya, A.; Mezza, B. J. Process for using catalyst with rapid formation of iron sulfide in slurry hydrocracking. U.S. Patent No. 8,277,638 B2, 2012.
- (30) Zhang, S.; Liu, D.; Deng, W.; Que, G. A Review of Slurry-Phase Hydrocracking Heavy Oil Technology. *Energy Fuels* **2007**, *21*, 3057–3062.
- (31) Speight, J. G. New approaches to hydroprocessing. *Catal. Today* **2004**, *98*, 55–60.
- (32) Pitault, I.; Fongarland, P.; Mitrovic, M.; Ronze, D.; Forissier, M. Choice of laboratory scale reactors for HDT kinetic studies or catalyst tests. *Catal. Today* **2004**, *98*, 31–42.
- (33) Angeles, M. J.; Leyva, C.; Ancheyta, J.; Ramírez, S. A review of experimental procedures for heavy oil hydrocracking with dispersed catalyst. *Catal. Today* **2014**, 220–222, 274–294.
- (34) Jafari, R.; Chaouki, J.; Tanguy, P. A., A Comprehensive Review of Just Suspended Speed in Liquid-Solid and Gas-Liquid-Solid Stirred Tank Reactors. *Int. J. Chem. React. Eng.* **2012**, 10.1015/1542-6580.2808
- (35) Sahu, R.; Song, B. J.; Im, J. S.; Jeon, Y.-P.; Lee, C. W. A review of recent advances in catalytic hydrocracking of heavy residues. *J. Ind. Eng. Chem.* **2015**, *27*, 12–24.
- (36) Raghava Rao, K.; Rewatkar, V.; Joshi, J. Critical impeller speed for solid suspension in mechanically agitated contactors. *AIChE J.* **1988**, *34*, 1332–1340.
- (37) Myers, K. J.; Fasano, J. B.; Corpstein, R. R. The influence of solid properties on the just-suspended agitation requirements of pitched-blade and high-efficiency impellers. *Can. J. Chem. Eng.* **1994**, *72*, 745–748.
- (38) Castañeda, L. C.; Muñoz, J. A. D.; Ancheyta, J. Combined process schemes for upgrading of heavy petroleum. *Fuel* **2012**, *100*, 110–127.
- (39) Reyniers, G. C.; Froment, G. F.; Kopinke, F.-D.; Zimmermann, G. Coke Formation in the Thermal Cracking of Hydrocarbons. 4. Modeling of Coke Formation in Naphtha Cracking. *Ind. Eng. Chem. Res.* **1994**, *33*, 2584–2590.
- (40) Towfighi, J.; Sadrameli, M.; Niaei, A. Coke formation mechanisms and coke inhibiting methods in pyrolysis furnaces. *J. Chem. Eng. Jpn.* **2002**, *35*, 923–937.
- (41) Gawel, I.; Bociarska, D.; Biskupski, P. Effect of asphaltenes on hydroprocessing of heavy oils and residua. *Appl. Catal., A* **2005**, *295*, 89–94.
- (42) Spiecker, P. M.; Gawrys, K. L.; Trail, C. B.; Kilpatrick, P. K. Effects of petroleum resins on asphaltene aggregation and water-in-oil emulsion formation. *Colloids Surf., A* **2003**, *220*, 9–27.
- (43) Bartholdy, J.; Lauridsen, R.; Mejlholm, M.; Andersen, S. I. Effect of hydrotreatment on product sludge stability. *Energy Fuels* **2001**, *15*, 1059–1062.
- (44) Bartholdy, J.; Andersen, S. I. Changes in asphaltene stability during hydrotreating. *Energy Fuels* **2000**, *14*, 52–55.
- (45) Gray, M. R. *Upgrading Petroleum Residues and Heavy Oil*; Marcel Dekker: New York, 1994.
- (46) Rankel, L. A. Hydrocracking vacuum resid with Ni/W bifunctional slurry catalysts. *Fuel Process. Technol.* **1994**, *37*, 185–202.
- (47) Weissman, J. G. Review of processes for downhole catalytic upgrading of heavy crude oil. *Fuel Process. Technol.* **1997**, *50*, 199–213.
- (48) Bockrath, B.; Lacount, R.; Kern, D.; Parfitt, D.; Frommell, E.; Keller, M. Characterization of unsupported MoS<sub>2</sub> catalysts by controlled atmosphere programmed-temperature oxidation. *Prepr. Symp.-Am. Chem. Soc., Div. Fuel Chem.* **1998**, *43*, 717–721.
- (49) Rezaei, H.; Ardakani, S. J.; Smith, K. J. Comparison of MoS<sub>2</sub> Catalysts Prepared from Mo-Micelle and Mo-Octoate Precursors for Hydroconversion of Cold Lake Vacuum Residue: Catalyst Activity, Coke Properties and Catalyst Recycle. *Energy Fuels* **2012**, *26*, 2768–2778.
- (50) Breyse, M.; Furimsky, E.; Kasztelan, S.; Lacroix, M.; Perot, G. Hydrogen activation by transition metal sulfides. *Catal. Rev.: Sci. Eng.* **2002**, *44*, 651–735.
- (51) Kasztelan, S.; McGarvey, G. B. Hydrogen content and hydrogenation activity of MoS<sub>2</sub>/γ-Al<sub>2</sub>O<sub>3</sub> and γ-Al<sub>2</sub>O<sub>3</sub> mechanical mixtures. *J. Catal.* **1994**, *147*, 476–483.
- (52) McGarvey, G. B.; Kasztelan, S. An investigation of the reduction behavior of MoS<sub>2</sub>/Al<sub>2</sub>O<sub>3</sub> and the subsequent detection of hydrogen on the surface. *J. Catal.* **1994**, *148*, 149–156.
- (53) Breyse, M.; Kasztelan, S. Catalytic hydrodesulfurization of automotive fuels. *Actual. Chim.* **2002**, *5*–6, 12–15.
- (54) Sun, M.; Adjaye, J.; Nelson, A. E. Theoretical investigations of the structures and properties of molybdenum-based sulfide catalysts. *Appl. Catal., A* **2004**, *263*, 131–143.
- (55) Omole, O.; Olieh, M. N.; Osinowo, T. Thermal visbreaking of heavy oil from the Nigerian tar sand. *Fuel* **1999**, *78*, 1489–1496.
- (56) Wu, C.; Lei, G.-L.; Yao, C.-j.; Sun, K.-j.; Gai, P.-y.; Cao, Y.-b. Mechanism for reducing the viscosity of extra-heavy oil by aquathermolysis with an amphiphilic catalyst. *J. Fuel Chem. Technol.* **2010**, *38*, 684–690.
- (57) Argillier, J.; Coustet, C.; Henaut, I. Heavy oil rheology as a function of asphaltene and resin content and temperature. In *2002 SPE International Thermal Operations & Heavy Oil Symposium*, November 4–7, 2002, Calgary, Alberta, Canada; Society of Petroleum Engineers: Richardson, TX, 2002; SPE-79496-MS.
- (58) Altgelt, K. H.; Harle, O. L. The Effect of Asphaltenes on Asphalt Viscosity. *Ind. Eng. Chem. Prod. Res. Dev.* **1975**, *14*, 240–246.
- (59) Zhang, H. Q.; Sarica, C.; Pereyra, E. Review of High-Viscosity Oil Multiphase Pipe Flow. *Energy Fuels* **2012**, *26*, 3979–3985.
- (60) Weitkamp, J. Catalytic Hydrocracking-Mechanisms and Versatility of the Process. *ChemCatChem* **2012**, *4*, 292–306.
- (61) Luo, P.; Gu, Y. Effects of asphaltene content on the heavy oil viscosity at different temperatures. *Fuel* **2007**, *86*, 1069–1078.
- (62) Hongfu, F.; Yongjian, L.; Liying, Z.; Xiaofei, Z. The study on composition changes of heavy oils during steam stimulation processes. *Fuel* **2002**, *81*, 1733–1738.
- (63) Rhoe, A.; Deblignieres, C. VISBREAKING - FLEXIBLE PROCESS. *Hydrocarbon Process* **1979**, *58*, 131–136.
- (64) Dealy, J. M. Rheological properties of oil sand bitumens. *Can. J. Chem. Eng.* **1979**, *57*, 677–683.
- (65) Reynolds, J. G. Modeling hydrodesulfurization, hydrodenitrogenation and hydrodemetalation. *Chem. Ind.* **1991**, *16*, 570–574.
- (66) Mitchell, P. C. H.; Scott, C. E. Interaction of vanadium and nickel porphyrins with catalysts, relevance to catalytic demetallisation. *Catal. Today* **1990**, *7*, 467–477.
- (67) Mitchell, P. C. H. Hydrodemetallisation of crude petroleum: fundamental studies. *Catal. Today* **1990**, *7*, 439–445.
- (68) Panariti, N.; Del Bianco, A.; Del Piero, G.; Marchionna, M.; Carniti, P. Petroleum residue upgrading with dispersed catalysts: Part 2. Effect of operating conditions. *Appl. Catal., A* **2000**, *204*, 215–222.
- (69) Gray, M.; Choi, J.; Egiebor, N.; Kirchen, R.; Sanford, E. Structural group analysis of residues from Athabasca bitumen. *Fuel Sci. Technol. Int.* **1989**, *7*, 599–610.
- (70) Li, Q.; Newberg, J. T.; Walter, E. C.; Hemminger, J. C.; Penner, R. M. Polycrystalline Molybdenum Disulfide (2H-MoS<sub>2</sub>) Nano- and Microribbons by Electrochemical/Chemical Synthesis. *Nano Lett.* **2004**, *4*, 277–281.



- (71) Nath, M.; Govindaraj, A.; Rao, C. N. R. Simple synthesis of MoS<sub>2</sub> and WS<sub>2</sub> nanotubes. *Adv. Mater.* **2001**, *13*, 283–286.
- (72) Wilcoxon, J. P.; Newcomer, P. P.; Samara, G. A. Synthesis and optical properties of MoS<sub>2</sub> and isomorphous nanoclusters in the quantum confinement regime. *J. Appl. Phys.* **1997**, *81*, 7934–7944.
- (73) Feldman, Y.; Wasserman, E.; Srolovitz, D. J.; Tenne, R. High-rate gas-phase growth of MoS<sub>2</sub> nested inorganic fullerenes and nanotubes. *Science* **1995**, *267*, 222–225.
- (74) Kaneko, T.; Tazawa, K.; Koyama, T.; Satou, K.; Shimasaki, K.; Kageyama, Y. Transformation of iron catalyst to the active phase in coal liquefaction. *Energy Fuels* **1998**, *12*, 897–904.
- (75) Shah, N.; Zhao, J. M.; Huggins, F. E.; Huffman, G. P. In situ XAFS spectroscopic studies of direct coal liquefaction catalysts. *Energy Fuels* **1996**, *10*, 417–420.
- (76) Nakao, Y.; Yokoyama, S.; Maekawa, Y.; Kaeriyama, K. Coal liquefaction by colloidal iron sulfide catalyst. *Fuel* **1984**, *63*, 721–722.
- (77) Mochida, I.; Sakanishi, K.; Suzuki, N.; Sakurai, M.; Tsukui, Y.; Kaneko, T. Progresses of coal liquefaction catalysts in Japan. *Catal. Surv. Jpn.* **1998**, *2*, 17–30.
- (78) Vasireddy, S.; Morreale, B.; Cugini, A.; Song, C.; Spivey, J. J. Clean liquid fuels from direct coal liquefaction: chemistry, catalysis, technological status and challenges. *Energy Environ. Sci.* **2011**, *4*, 311–345.
- (79) Kaneko, T.; Tazawa, K.; Okuyama, N.; Tamura, M.; Shimasaki, K. Effect of highly dispersed iron catalyst on direct liquefaction of coal. *Fuel* **2000**, *79*, 263–271.
- (80) Peureux, S.; Bonnamy, S.; Fixari, B.; Lambert, F.; Le Perche, P.; Pepin-Donat, B.; Vrinat, M. Deep Hydroconversion of Heavy Oil Residues with Dispersed Catalysts: Analysis of the Transformation. *Bull. Soc. Chim. Belg.* **1995**, *104*, 359–366.
- (81) Shuyi, Z.; Wenan, D.; Hui, L.; Dong, L.; Guohe, Q. Slurry-phase residue hydrocracking with dispersed nickel catalyst. *Energy Fuels* **2008**, *22*, 3583–3586.
- (82) Sanford, E. C. Conradson Carbon Residue Conversion during Hydrocracking of Athabasca Bitumen: Catalyst Mechanism and Deactivation. *Energy Fuels* **1995**, *9*, 549–559.
- (83) Liu, D.; Li, M. Y.; Deng, W. A.; Que, G. H. Reactivity and Composition of Dispersed Ni Catalyst for Slurry-Phase Residue Hydrocracking. *Energy Fuels* **2010**, *24*, 1958–1962.
- (84) Termeer, C. *Fundamentals of Investing in Oil and Gas*; Chris Termeer: Clearwater Beach, FL, 2013.
- (85) Ellis, P. J.; Paul, C. A.; Session, T. Tutorial: Delayed coking fundamentals. In *AIChE 1998 Spring National Meeting Topical Conference on Refinery Processing*, New Orleans, LA, March 8–12, 1998; Tutorial Session: Delayed Coking, Paper 29a.
- (86) Marsh, H.; Calvert, C.; Bacha, J. Structure and formation of shot coke—a microscopy study. *J. Mater. Sci.* **1985**, *20*, 289–302.
- (87) Reis, T. To coke, desulfurize and calcine. Part 2: coke quality and its control. *Hydrocarbon Process.* **1975**, *54* (6), 97–104.
- (88) Jakob, R. R. Coke quality and how to make it. *Hydrocarbon Process.* **1971**, *50*, 132–136.